RSC Advances

PAPER

View Article Online
View Journal | View Issue

Cite this: *RSC Adv.*, 2017, **7**, 8512

Anti-neuroinflammatory asarone derivatives from the rhizomes of *Acorus tatarinowii*†

Da-Peng Qin,‡[a] Xiao-Lin Feng,‡[a] Wei-Yang Zhang,[d] Hao Gao,[a] Xiao-Rui Cheng,[c] Wen-Xia Zhou,[c] Yang Yu*[ab] and Xin-Sheng Yao*[a]

Received 5th December 2016
Accepted 8th January 2017

DOI: 10.1039/c6ra27786a

www.rsc.org/advances

A novel 7-*O*-7′ type mesomeric neolignan, *meso*-asarolignan A (**1**), six pairs of new neolignan enantiomers, (±)-asarolignan B–G (**2a/2b**, **3a/3b**, **4**–**6**, **7a/7b**), along with 16 known analogues (**8**–**23**) were isolated from the rhizomes of *Acorus tatarinowii*. The structures of the new compounds were elucidated by extensive analysis of spectroscopic, X-ray diffraction, and computational data. Compounds **1**–**3** represent rare examples of naturally occurring lignans with a 7-*O*-7′ linkage pattern. All isolated compounds were assayed for their anti-neuroinflammatory effects on tumor necrosis factor α (TNF-α) production in an activated murine microglia cell line. Compounds **7(a/b)**, **14(a/b)**, **16**, **20**, and **22** reduced TNF-α levels without high cell toxicity in LPS-activated BV-2 cells.

Introduction

Acorus tatarinowii has been historically used as a principal medicine in traditional Chinese formulas for the treatment of learning and memory disorders, dementia and dysmnesia.[1,2] Previous studies on *Acorus tatarinowii* have revealed that the most notable constituents are α- and β-asarones, which exhibit a wide spectrum of biological activities, such as cerebrovascular protection, anticancer, antioxidation, neuroprotection, anti-neuroinflammation, improving cognitive function, antidepressant-like effects and antibacterial activity.[3–8]

Over the course of our continuing investigations on bioactive asarone analogues from the rhizomes of *Acorus tatarinowii*, 14 neolignans (**1**–**7**, **9**–**15**), one quinone (**8**), six asarone analogues (**16**–**21**), along with α- and β-asarones (**22** and **23**) were isolated. Interestingly, compounds **1**–**3** were obtained as stereoisomers, represented the first examples of naturally occurring 7-*O*-7′ type neolignans. *meso*-Asarolignan A (**1**) was defined as a mesomer, while (±)-asarolignan B (**2**) and C (**3**) were two pairs of 7-*O*-7′ neolignan enantiomers. The resolution of enantiomers **2** and **3** by chiral HPLC led to the isolation of **2a/2b** and **3a/3b**. Considering the racemic nature of the compounds from this plant, compounds **3**–**8** were also determined as racemic mixtures due to their negligible optical activities. In addition, all isolated compounds were assayed for their anti-neuroinflammatory effects on tumor necrosis factor α (TNF-α) production in the murine microglia BV-2 cells.

Results and discussion

Compound **1** was obtained as colourless block crystal. Its molecular formula was determined to be $C_{24}H_{34}O_9$ by HRESIMS at *m*/*z* 489.2094 $[M + Na]^+$ (calcd 489.2101). The UV spectrum exhibited absorption maxima at 205, 231 (sh) and 291 nm. Its IR spectrum disclosed absorption bands assignable to hydroxyl (3378 cm^{-1}) and benzene ring moiety (1614, 1512, and 1465 cm^{-1}). The ^1H NMR spectrum of **1** (Table 1) showed the signals for a 1,2,4,5-tetrasubstituted benzene ring [δ_H 6.67 (s, H-6/6′), 6.41 (s, H-3/3′)], two oxygenated methines [δ_H 4.57 (d, $J = 7.9$ Hz, H-7/7′), 3.88 (m, H-8/8′)], one methyl [δ_H 0.92 (d, $J = 6.4$ Hz, Me-9/9′)] and three methoxy groups [δ_H 3.76, 3.62, 3.56 (each 3H, s)]. The ^{13}C NMR in combination with DEPT135 experiments resolved 12 carbon signals, corresponding to six aromatic carbons, two oxygenated methine carbons, one methyl, and three methoxy groups. These data together with the molecular formula could make us assume that **1** might be a highly symmetrical structure. Further analysis of the ^1H–^1H COSY, HSQC and HMBC spectra allowed the establishment of the partial C_6–C_3 moiety (1′,2′-dihydroxyasarone moiety, half of the structure) in compound **1** (Fig. 4). The large coupling constant between H-7 (H-7′) and H-8 (H-8′) ($J = 7.9$ Hz) indicated a *threo* relative configuration. Connection of the two C_6–C_3 units in **1** was mainly carried out by using the results of HMBC and X-ray analyses. The key HMBC correlations from H-7 to C-7′ or H-7′ to

[a]*Institute of Traditional Chinese Medicine & Natural Products, College of Pharmacy, Jinan University, Guangzhou 510632, P. R. China. E-mail: 1018yuyang@163.com; tyaoxs@jnu.edu.cn; Fax: +86-20-85221559; Tel: +86-20-85221559*

[b]*State Key Laboratory of Bioactive Substance and Function of Natural Medicines, Institute of Materia Medica, Chinese Academy of Medical Sciences and Peking Union Medical College, Beijing 100050, P. R. China*

[c]*Beijing Institute of Pharmacology and Toxicology, Beijing 100850, P. R. China*

[d]*State Key Laboratory of Quality Research in Chinese Medicine, Macau University of Science and Technology, Macau, P. R. China*

† Electronic supplementary information (ESI) available: NMR spectra of all new compounds. CCDC 1518425–1518428. For ESI and crystallographic data in CIF or other electronic format see DOI: 10.1039/c6ra27786a

‡ These authors have contributed equally to this work.

Table 1 ^{1}H NMR and ^{13}C NMR data for compounds **1–3**[a]

1			**2**		**3**					
No.	δ_C	δ_H (J in Hz)	δ_C	δ_H (J in Hz)	No.	δ_C	δ_H (J in Hz)	No.	δ_C	δ_H (J in Hz)
1,1′	121.9		120.4		1	120.5		1′	119.1	
2,2′	153.1		154.1		2	154.4		2′	154.3	
3,3′	98.7	6.41 (1H, s)	99.2	7.09 (1H, s)	3	99.0	6.62 (1H, s)	3′	99.3	6.62 (1H, s)
4,4′	150.5		150.7		4	150.9		4′	150.6	
5,5′	144.2		144.7		5	144.8		5′	144.5	
6,6′	114.4	6.67 (1H, s)	114.3	6.62 (1H, s)	6	113.8	7.01 (1H, s)	6′	115.3	7.19 (1H, s)
7,7′	83.0	4.57 (1H, d, 7.9)	77.0	4.35 (1H, d, 6.5)	7	77.3	4.39 (1H, d, 7.4)	7′	75.9	4.45 (1H, d, 3.2)
8,8′	73.1	3.88 (1H, m)	72.1	3.85 (1H, m)	8	72.4	3.85 (1H, m)	8′	71.3	3.98 (1H, m)
9,9′	18.8	0.92 (3H, d, 6.4)	19.1	0.94 (3H, d, 6.4)	9	18.9	0.91 (3H, d, 6.3)	9′	18.6	1.00 (3H, d, 6.6)
2,2′-OMe	56.8	3.76 (3H, s)	56.8	3.62 (3H, s)	2-OMe	56.8	3.61 (3H, s)	2′-OMe	56.8	3.61 (3H, s)
4,4′-OMe	57.2	3.56 (3H, s)	56.7	3.85 (3H, s)	4-OMe	56.9	3.85 (3H, s)	4′-OMe	55.7	3.85 (3H, s)
5,5′-OMe	56.8	3.62 (3H, s)	57.2	3.81 (3H, s)	5-OMe	57.4	3.80 (3H, s)	5′-OMe	57.2	3.83 (3H, s)

[a] Recorded at 400 (^{1}H) and 100 MHz (^{13}C) in CD_3OD. Multiplets or overlapped signals are reported without designating multiplicity.

C-7 indicated the linkage of the two C_6–C_3 units through C-7-*O*-C-7′ bonds. The fact that compound **1** bears four chiral centres and symmetric nature, was undoubtedly confirmed by X-ray (Fig. 2) using anomalous scattering of Mo Kα radiation. The crystals of **1** belong to monoclinic space group $P2_1/c$, showing a helical conformation with an intramolecular mirror symmetry. These findings, combined with the lack of optical activity supported that compound **1** was obtained as a mesomer. Therefore, the structure of **1** was established as a novel 7-*O*-7′ neolignan mesomer, and named *meso*-asarolignan A.

Compound **2** (**2a**/**2b**), obtained as a colourless block crystal, possesses the same molecular formula ($C_{24}H_{34}O_9$) as compound **1**, as determined by HREIMS [M + Na]$^+$ ion at m/z 489.2101 (calcd 489.2101). The NMR data of **2** (Table 1) were similar to those of **1**, except that broad signal of C-6/6′ was obviously observed at δ_C 114.3 ppm and the broad signal of oxygenated methine considerably upfield shifted to δ_C 77.0 ppm [δ_C 80.8 (C-7/7′) in **1**]. Similarly, the same C_6–C_3 moiety (1′,2′-dihydroxyasarone, Fig. 4) with a *threo* relative configuration was assigned in **2**. Crystals of **2** were obtained from CH_3OH–H_2O (9 : 1), which allowed the establishment of the structure of **2** by X-ray analysis (Fig. 2). Thus, **2** was unambiguously defined as a stereoisomer of **1**. The chiral HPLC and optical rotation data indicated that **2** was racemic mixture. Subsequent chiral resolution of **2** by HPLC yielded the enantiomers **2a** and **2b** in a 1 : 1 ratio. The enantiomers displayed typical antipodal ECD curves (Fig. 3) and specific rotations of opposite sign (**2a**: $[\alpha]_D^{23}$ +173; **2b**: $[\alpha]_D^{23}$ −174). Furthermore, the configuration of **2b** was determined as 7*S*,8*S*,7′*S*,8′*S* on the basis of the good agreement with calculated ECD spectra of (7*S*,8*S*,7′*S*,8′*S*)-**2**, and the configuration of **2a** was determined to be 7*R*,8*R*,7′*R*,8′*R*. Finally, the enantiomers **2a** and **2b** were named as (+)-asarolignan B and (−)-asarolignan B, respectively.

The molecular formula of compound **3** (**3a**/**3b**), $C_{24}H_{34}O_9$, was identical to those of **2**, as indicated by HRESIMS at m/z 489.2103 [M + Na]$^+$ (calcd 489.2101). The NMR data of **3** (Table 1) were similar to those of **2**, except that two sets of signals for C_6–C_3 units were distinctly observed in **3**. A detailed comparison and analyses of the NMR data of **3** revealed the establishment of two same C_6–C_3 moieties (1′,2′-dihydroxyasarone, Fig. 4). The relative configurations were assigned as 7,8-*threo* and 7′,8′-*erythro* due to the observed coupling constants of H-7/H-8 ($J_{7,8}$ = 7.4 Hz) and H-7′/H-8′ ($J_{7',8'}$ = 3.2 Hz), respectively. Thus, the structure of **3** was defined as a stereoisomer of **2** with different relative configurations as shown in Fig. 1. Similarly, the enantiomers (+)-**3a** and (−)-**3b** were obtained and showed opposite ECD curves and optical rotations of opposite sign. Comparing the CD spectra of **2** (**a**/**b**) and **3** (**a**/**b**) in Fig. 3, the configurations of **3a** and **3b** were determined to be 7*R*,8*S*,7′*R*,8′*R* and 7*S*,8*R*,7′*S*,8′*S*, respectively. Thus, two enantiomers of **3** were assigned as (+)-asarolignan C (**3a**) and (−)-asarolignan C (**3b**).

(±)-Asarolignan D (**4**), white solid, was assigned molecular formula $C_{25}H_{36}O_7$ by HRESIMS (m/z 471.2363, [M + Na]$^+$) with eight degrees of unsaturation. The IR spectrum showed the presence of aromatic ring (1509, and 1458 cm^{-1}). The NMR data of **4** (Table 2) showed four aromatic proton signals at [δ_H 6.86 (1H, s, H-6), 6.84 (1H, s, H-6′), 6.68 (1H, s, H-3′), and 6.64 (1H, s, H-3)], which were ascribed to the protons of two tetrasubstituted aromatic rings. Moreover, three methines groups [δ_H 4.22 (1H, d, J = 3.5 Hz, H-7), 3.04 (1H, br s, H-7′), 1.94 (1H, m, H-8)], one methylene [δ_H 1.78 (1H, m, H-8′a), 1.52 (1H, m, H-8′b)], two methyls [δ_H 0.84 (3H, d, J = 7.0 Hz, Me-9), and 0.65 (3H, t, J = 7.4 Hz, Me-9′)], and seven methoxy groups [δ_H 3.83, 3.81, 3.80, 3.78, 3.75, 3.70, 2.99 (each 3H, s)] were also observed. The ^{1}H–^{1}H COSY spectrum showed two spin coupling systems arising from two C_3 substructures (C-7–C-8–C-9 and C-7′–C-8′–C-9′) shown in bold lines in Fig. 4. In the HMBC spectrum, correlations from H-6 to C-7, H-7 to C-1/C-2/C-6, H-6′ to C-7′, and H-8′a to C-1′, allowed the establishment of two C_6–C_3 units. Furthermore, the ^{1}H–^{1}H COSY correlations from H-8 to H-7′, together with the key HMBC correlations from Me-9 to C-7/C-7′, and H-8 to C-1′/C-8′, indicated the two C_6–C_3 units were connected *via* C-8–C-7′ bond form a neolignan (Fig. 4). A methoxy group at δ_H 2.99 was located at C-7 as confirmed by the HMBC correlation from MeO-7 to C-7. The remaining six methoxy resonances were unambiguously located on the aromatic rings

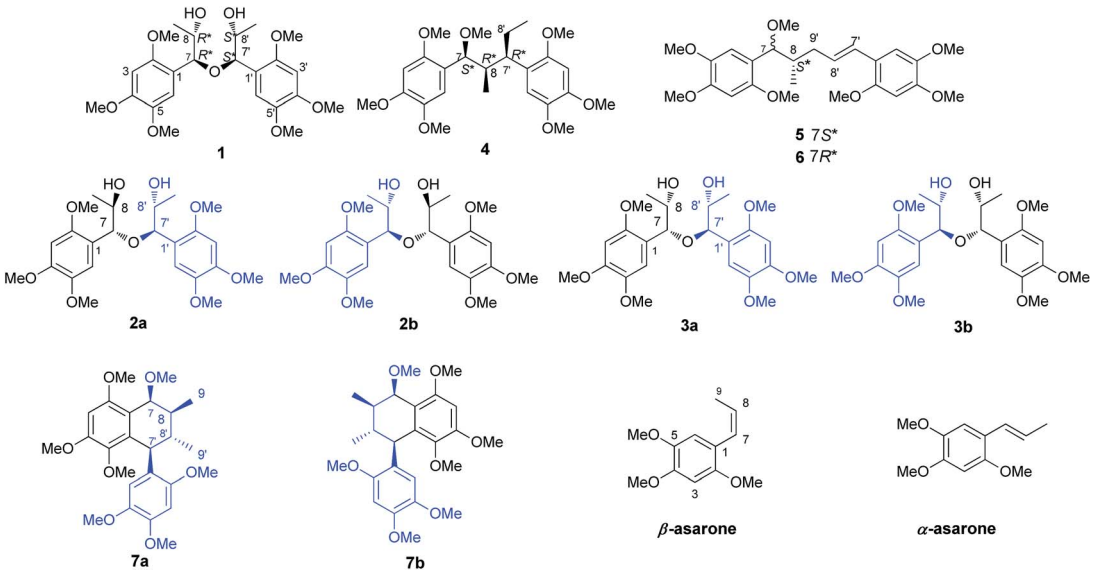

Fig. 1 Chemical structures from the rhizomes of *A. tatarinowii*.

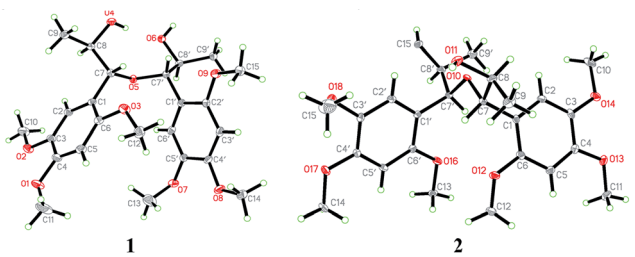

Fig. 2 X-ray crystallographic structures of **1** and **2**.

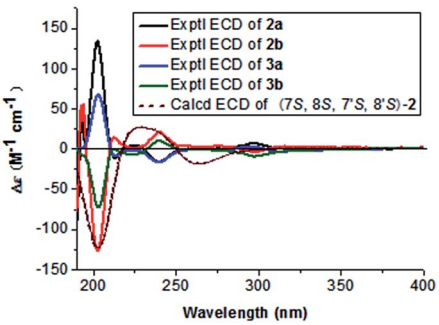

Fig. 3 Experimental ECD spectra of **2a**, **2b** and **3a**, **3b**, and calculated ECD spectrum of (7*S*,8*S*,7′*S*,8′*S*)-**2**.

by using the HMBC and NOE experiments. Finally, an X-ray diffraction analysis was performed, from which the relative configuration of **4** (7*S**,8′*R**,7′*R**) was determined (Fig. 5). The lack of optical activity suggested that **4** was obtained as a racemate. Attempts to separate the enantiomers of **4** using different chiral phase columns were not successful.

(±)-Asarolignan E (**5**), colourless oil, was assigned the molecular formula $C_{25}H_{34}O_7$ by HRESIMS (*m*/*z* 469.2203, [M + Na]$^+$) with nine degrees of unsaturation. The ^{1}H and ^{13}C NMR data (Table 2) indicated its structural similarity to **4**, except for the replacement of a methine and a methylene groups by two olefinic carbons. By ^{1}H–^{1}H COSY, HSQC, and HMBC spectra, two C_6–C_3 units were assigned as shown in Fig. 4. Similarly, the connection between C-8 and C-9′ was determined as the correlations from Me-9 to C-7/C-9′, H-7 to C-9′, and H-9′ to C-8/C-9/C-7′. The large coupling constant of H-7/H-8 ($J_{7,8}$ = 7.6 Hz), indicated a *threo* relative configuration. On the basis of the negligible optical activity, compound **5** was also deduced as a racemic mixture and named as (±)-asarolignan E.

(±)-Asarolignan F (**6**), colourless oil, had the same molecular formula as **5**, established by HRESIMS. The ^{1}H and ^{13}C NMR spectroscopic data of **6** (Table 2) indicated them to be very similar to **5**, differing only in the relative configurations at C-7/8. The coupling constant of H-7/H-8 was 6.1 Hz, which suggested that the configuration was *erythro* in comparison with a higher value in *threo* ($J_{7,8}$ = 7.6 Hz) configuration of **5**. Thus, **6** was identified as (±)-asarolignan F.

(±)-Asarolignan G (**7**) was obtained as yellow oil. Its molecular formula was assigned $C_{25}H_{34}O_7$ by HRESIMS (*m*/*z* 469.2196, [M + Na]$^+$) with nine degrees of unsaturation. The ^{13}C NMR and DEPT-135 spectra exhibited 25 carbon signals, corresponding to two aromatic rings, four methines, two methyls and seven methoxy groups. Based on these data, the skeleton of **7** was speculated to be a lignan with seven methoxy substitutes. The ^{1}H–^{1}H COSY spectrum suggested the presence of H-7/H-8/H-9, H-7′/H-8′/H-9′ and H-8/H-8′ units (bold lines in Fig. 6), and the HMBC correlations of H-7 to C-1/C-2/C-6/C-8′, and H-7′ to C-1′/C-2′/C-6′/C-1/C-5/C-6, were indicative of a tetrahydronaphthalene lignan structure. The other six methoxy groups linked to two substituted aromatic rings by HMBC and NOE experiments, respectively (Fig. 6). Furthermore, the coupling constant of H-7/H-8 ($J_{7,8}$ = 1.9 Hz) and H-7′/H-8′ ($J_{7',8'}$ = 8.7 Hz), demonstrated the *cis* and *trans* relative configurations of H-7/H-8 and H-7′/H-8′, respectively. In the NOESY spectrum, the correlations of Me-

Table 2 ^{1}H NMR and ^{13}C NMR data for compounds **4–8**

	4[a]		**5**[b]		**6**[c]		**7**[b]	
No.	δ_C	δ_H (J in Hz)	δ_C	δ_H (J in Hz)	δ_C	δ_H (J in Hz)	δ_C	δ_H (J in Hz)
1	122.5		122.0		122.0		120.5	
2	152.7		154.1		153.8		155.1	
3	99.2	6.64 (1H, s)	99.7	6.58 (1H, s)	99.4	6.58 (1H, s)	96.0	6.55 (1H, s)
4	150.0		150.6		150.4		154.3	
5	144.2		144.7		144.5		141.8	
6	113.7	6.86 (1H, s)	113.2	6.87 (1H, s)	113.1	6.87 (1H, s)	137.9	
7	79.7	4.22 (1H, d, 3.5)	82.0	4.39 (1H, d, 7.6)	81.6	4.44 (1H, d, 6.1)	76.2	4.55 (1H, d, 1.9)
8	43.3	1.94 (1H, m)	40.9	1.90 (1H, m)	40.6	1.88 (1H, m)	42.0	1.37 (1H, m)
9	11.8	0.84 (3H, d, 7.0)	16.2	0.75 (3H, d, 6.9)	15.9	0.94 (3H, d, 6.6)	17.2	1.10 (1H, d, 6.8)
1′	125.2		120.6		120.3		131.0	
2′	153.9		152.6		152.5		152.9	
3′	99.2	6.68 (1H, s)	99.1	6.64 (1H, s)	98.9	6.62 (1H, s)	99.1	6.65 (1H, s)
4′	149.3		150.6		150.5		144.6	
5′	144.2		144.8		144.6		148.8	
6′	115.9	6.84 (1H, s)	112.1	6.96 (1H, s)	111.7	6.92 (1H, s)	115.5	6.58 (1H, s)
7′	43.3	3.04 (1H, br s)	126.5	6.57 (1H, d, 14.7)	126.1	6.50 (1H, d, 15.9)	41.8	4.16 (1H, d, 8.7)
8′	25.3	1.78 (1H, m), 1.52 (1H, m)	128.7	6.03 (1H, dt, 14.7, 6.5)	128.7	5.90 (1H, dt, 15.9, 7.1)	39.5	1.86 (1H, m)
9′	12.7	0.65 (3H, t, 7.4)	37.8	2.53 (1H, m), 2.06 (1H, m)	38.7	2.18 (1H, m), 2.00 (1H, m)	18.1	0.93 (3H, d, 6.7)
7-OMe	57.3	2.99 (3H, s)	57.0	3.15 (3H, s)	57.1	3.16 (3H, s)	57.7	3.45 (3H, s)
2-OMe	56.4	3.70 (3H, s)	57.1	3.77 (3H, s)	57.0	3.78 (3H, s)	56.7	3.85 (3H, s)
4-OMe	56.5	3.81 (3H, s)	56.7	3.83 (3H, s)	56.7	3.81 (3H, s)	56.7	3.79 (3H, s)
5-OMe	57.6	3.75 (3H, s)	57.5	3.76 (3H, s)	57.4	3.77 (3H, s)	57.0	3.06 (3H, s)
2′-OMe	56.5	3.78 (3H, s)	56.8	3.77 (3H, s)	56.7	3.77 (3H, s)	56.7	3.88 (3H, s)
4′-OMe	57.2	3.83 (3H, s)	56.7	3.81 (3H, s)	56.6	3.81 (3H, s)	57.0	3.58 (3H, s)
5′-OMe	56.5	3.80 (3H, s)	57.4	3.76 (3H, s)	57.4	3.71 (3H, s)	56.7	3.81 (3H, s)

[a] Recorded at 600 (^{1}H) and 125 MHz (^{13}C) in acetone-d_6. [b] Recorded at 400 (^{1}H) and 100 MHz (^{13}C) in CD_3OD. [c] Recorded at 300 (^{1}H) and 75 MHz (^{13}C) in CD_3OD. Multiplets or overlapped signals are reported without designating multiplicity.

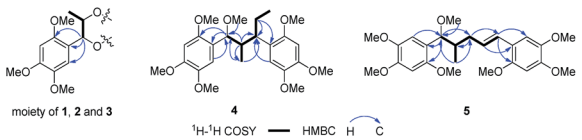

Fig. 4 Key ^{1}H–^{1}H COSY and HMBC correlations of **1–5**.

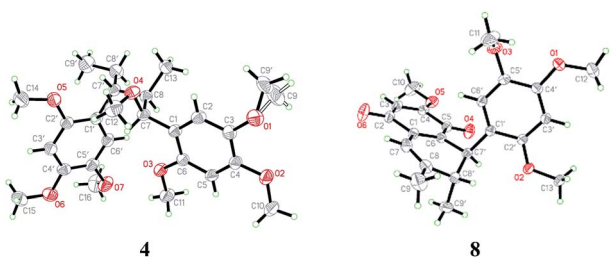

Fig. 5 X-ray crystallographic structure of **4** and **8**.

9 and MeO-7, H-8 and H-7′, as well as Me-9′ and H-7′ suggested that H-7, H-8 and H-7′ were β-oriented, whereas H-8′ was situated on the opposite side. Considering the racemic nature, chiral HPLC analysis was performed and the resolved enantiomers (**7a** and **7b**) possessed the opposite CD curves (Fig. 7). The absolute configuration of **7a** was determined as 7*S*,8*S*,7′*S*,8′*R* by the CD data showing a negative Cotton effect at 285 nm. Similarly, the absolute configuration of **7b** was elucidated as 7*R*,8*R*,7′*R*,8′*S*. Thus, two enantiomers were established and named as (+)-asarolignan G and (−)-asarolignan G, respectively.

The remaining known compounds, including acortatarinowin H (**8**),[9] tatarinan A (**9**),[10] magnosalin (**10**),[11] andamanicin (**11**),[11] 5,5′-((1*R**,2*R**,3*R**,4*S**)-3,4-dimethylcyclobutane-1,2-diyl) bis(1,2,4-trimethoxybenzene) (**12**),[12] magnoshinin (**13**),[13] tatarinoid C (**14**),[14] and tatanan C (**15**),[15] (7*R**,8*S**)-7,8-dihydroxyasarone (**16**),[16,17] (7*S**,8*S**)-7,8-dihydroxyasarone (**17**),[16,17] (7*R**,8*S**)-(7-methoxy-8-hydroxy)-asarone (**18**),[16,17] (7*S**,8*S**)-(7-

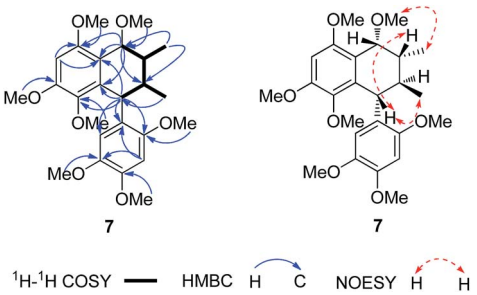

Fig. 6 Selected ^{1}H–^{1}H COSY, HMBC and NOE correlations of **7**.

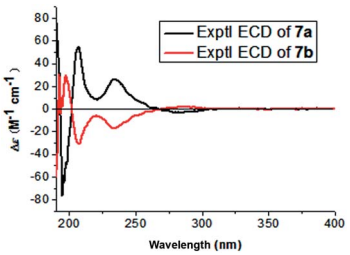

Fig. 7 Experimental ECD spectra of 7a, 7b.

methoxy-8-hydroxy)-asarone (**19**),[16,17] isoacoramone (**20**),[18] asaraldehyde (**21**),[18] β-asarone (**22**)[19] and α-asarone (**23**)[19] were identified by comparison of their physiochemical properties and spectral data with those reported in the literature. Among them, the known compound (±)-acortatarinowin H (**8**) was obtained as red-brown block crystals, the X-ray diffraction experiment showed an unambiguous assignment of the configurations as 7′*S**,8′*R** (Fig. 5). It was worth noting that the crystals of **8** had a $P2_1/n$ space group, indicating a racemic nature, which was in accordance with its small optical value {$[\alpha]_D^{23}$ 0 (*c* 0.5, MeOH)}. Subsequent chiral resolution was performed on a chiral column to yield **8a** and **8b**, which were opposite in terms of ECD curves (see ESI†). The absolute configurations of **8a** and **8b** were determined as (7′*S*,8′*R*) and (7′*R*,8′*S*), respectively, by comparing their cotton effects at 280–300 nm in CD spectra with those reported in the literatures.[20,21] Tatarinoid C (**14**) was firstly separated by chiral HPLC analysis. Compared with calculated ECD spectra of (8*R*)-**14**, the two enantiomers named as (+)-tatarinoid C (**14a**) and (−)-tatarinoid C (**14b**), respectively (see ESI†).

Pharmacological studies have indicated that neuroinflammation plays a major role such as dysregulation of genes in the pathophysiology of Alzheimer's disease (AD) and Parkinson's disease (PD).[22] TNF-α is one of the critical proinflammatory cytokines.[23,24] To a certain extent, reducing TNF-α levels has the potential to medicate anti-neuroinflammation action. In our study, all the isolated compounds were evaluated for anti-neuroinflammatory activities on TNF-α production in LPS-activated BV-2 cells. As shown in Fig. 8, compounds **7a**, **7b**, **14a**, **14b**, **16**, **20**, and **22** could reduce TNF-α levels in the murine microglia BV-2 cells. A comparison of the inhibition of the enantiomers 7 (**7a**/**7b**), and **14** (**14a**/**14b**) in this assay, suggested the configuration was not critical to the anti-neuroinflammation activity. In addition, all the compounds were assayed for cytotoxicity against BV-2 cells by CCK-8 method, and α-asarone (**23**) displayed cytotoxicity at 20 and 50 μM.

Conclusions

In summary, twenty-three compounds derived from asarone biogenetic pathway were isolated and identified from the rhizomes of *Acorus tatarinowii*, including seven new neolignans (**1**–**7**). Their structures including absolute configurations were determined by comprehensive spectroscopic data together with X-ray crystallography, as well as experimental and calculated ECD spectra. Besides, all the compounds were evaluated for anti-neuroinflammatory activities on TNF-α production in LPS-activated BV-2 cells. INDO (indomethacin, 10 μM) and DEX (dexamethasone, 10 μM) were used as positive control. As results, compounds **7**, **7a**, **7b**, **14b** and **16** exhibited obvious inhibitory effects on the release of TNF-α at a concentration of 50 μM, their TNF-α level were 1.7, 2.0, 1.9, 2.5 and 2.6 μg mL^{-1}, respectively; compound **20** could inhibit the release of TNF-α at a concentration of 20 μM (TNF-α level was 2.5 μg mL^{-1}) and 50 μM (TNF-α level was 2.1 μg mL^{-1}); compound **22** could dramatically reduce TNF-α level at a concentration of 5 μM (TNF-α level was 2.8 μg mL^{-1}) and 50 μM (TNF-α level was 2.6 μg mL^{-1}). These findings will provide some scientific foundation for the utilization of *Acorus tatarinowii* as CNS disorders treatment.

Experimental

General experimental procedures

Optical rotations were measured on a JASCO P-1020 polarimeter with a 1 cm cell at room temperature. UV spectra were recorded on a JASCO V-550 UV/Vis spectrometer. IR spectra were obtained using a JASCO FT/IR-480 plus spectrometer. CD spectra were obtained on a JASCO J-810 spectropolarimeter at room

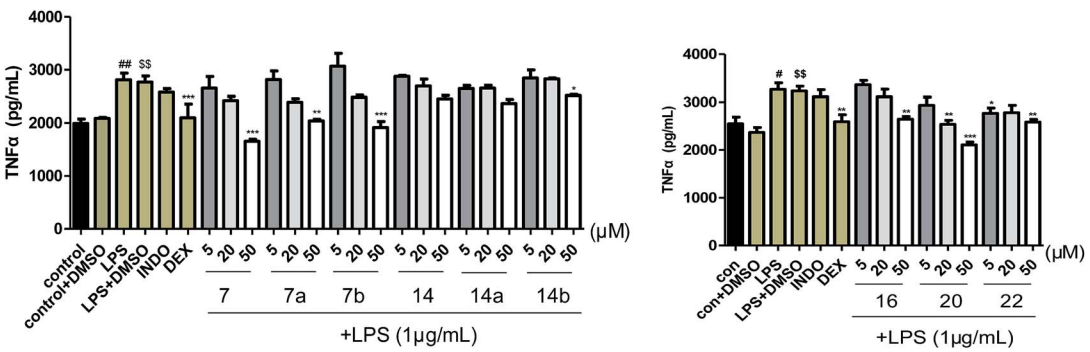

Fig. 8 Compounds 7, 7a, 7b, 14, 14a, 14b, 16, 20, 22 inhibit TNF-α levels in the murine microglia BV-2 cells. Results are expressed as mean ± SEM and include data from three independent experiments performed in triplicate. $^{\#}p < 0.05$, $^{\#\#}p < 0.01$, when compared to the control group, $^{\$\$}p < 0.01$, when compared to the control + DMSO group, and $^{*}P < 0.05$, $^{**}P < 0.01$, $^{***}P < 0.001$, when compared to the LPS + DMSO group.

temperature. HRESIMS spectra were acquired using a Waters Synapt G2 mass spectrometer. 1D and 2D NMR data were acquired with Bruker AV 600, and AV 400 using solvent signals ($CDCl_3$: δ_H 7.26/δ_C 77.0; DMSO-d_6: δ_H 2.50/δ_C 39.5) as the internal standard. Silica gel (200–300 mesh, Qingdao Marine Chemical Ltd., China), octadecyl silanized (ODS) silica gel (YMC Ltd., Japan), and Sephadex LH-20 (Amersham Pharmacia Biotech, Sweden) were used for column chromatography (CC). TLC was performed on precoated silica gel plate (SGF_{254}, 0.2 mm, Yantai Chemical Industry Research Institute, China). The analytical HPLC was performed on a Waters 2695 separations module equipped with a 2998 photodiode array detector using an RP-18 column (5 μm, 4.6 × 250 mm; COSMOSIL). Chiral semi-preparative HPLC was performed using a Lux Amylose-2 column (5 μm, 4.6 × 250 mm, Phenomenex). The semi-preparative and preparative HPLC were carried on a Waters 1515 isocratic HPLC pump equipped with a 2489 UV/Vis detector and RP-18 columns (5 μm, 10 × 250 mm; 5 μm, 20 × 250 mm; COSMOSIL).

Plant material

The dried rhizomes of *Acorus tatarinowii* were purchased from PuraPharm Corporation in 2011 and identified by Jia-Fu Wei, the pharmacist of Guangxi Institute for Food and Drug Control, China. A voucher specimen (20110301) was deposited in the Institute of Traditional Chinese Medicine & Natural Products, Jinan University, Guangzhou, P. R. China.

Extraction and isolation

The air-dried and powdered rhizomes of *Acorus tatarinowii* (19.5 kg) were refluxed with 60% EtOH for 2 h (×2) to give an crude extract (2.2 kg), which was suspended in water (10 L) followed by an exhaustive partition with EtOAc and *n*-BuOH. The EtOAc soluble extract (312.0 g) was separated by silica gel CC (ϕ 12.0 × 36.0 cm) eluted with gradient cyclohexane–EtOAc (100 : 0 → 0 : 100) to afford seven fractions (Fr. 1–7). Fr. 2 (144.9 g) was fractionated further by silica gel CC (ϕ 2.5 × 54.0 cm) eluted gradiently with ether–acetone (100 : 1, 98 : 2, 95 : 5 and 0 : 100, v/v) to yield 8 fractions (Fr. 2.1–2.8). Fr. 2.3 (5.5 g) were purified by recrystallization from ether to afford compound **22** (5.4 g). Fr. 2.6 (4.2 g) was subjected to semipreparative RP-HPLC (65% MeOH–H_2O) to afford **23** (2.0 mg, t_R = 28.9 min) and **21** (100.0 mg, t_R = 35.0 min). Fr. 3 (22.9 g) was further purified by using ODS CC (ϕ 3.0 × 40.0 cm) eluted gradiently with MeOH–H_2O followed by semipreparative RP-HPLC (65% MeOH–H_2O) to afford compound **7** (10.9 mg, t_R = 42.7 min). Compound **7** was isolated using a chiral analytical column (60% MeCN–H_2O, 0.7 mL min^{-1}) to yield compounds **7a** (2.2 mg) and **7b** (2.2 mg). Fr. 4 (8.8 g) was further subjected to ODS CC (ϕ 3.3 × 25.0 cm) with a gradient system of MeOH–H_2O gradient (3 : 7, 1 : 1, 7 : 3, 8 : 2, 9 : 1 and 1 : 0, v/v) to afford 14 subfractions (Fr. 4.1–4.14). Fr. 4.2 (1.1 g) was separated by silica gel CC (ϕ 2.5 × 54.0 cm) eluted gradiently with cyclohexane–acetone (98 : 2 → 7 : 3) to yield 11 fractions (Fr. 4.2.1–4.2.11). Fr. 4.2.6 (78.3 mg) was subjected to RP-HPLC (55% MeOH–H_2O) to afford compound **20** (24.0 mg, t_R = 50.0 min). Fr. 4.3 (3.4 g) was separated by the same manner as Fr. 4.2 to give 16 fractions (Fr. 4.3.1–4.3.16). Compound **10** (40.4 mg, t_R = 25.2 min) was obtained by RP-HPLC eluted with 65% MeOH–H_2O from Fr. 4.3.9 (961.3 mg). Fr. 4.4 (840.4 mg) was separated by the same manner as Fr. 4.2 to yield 9 fractions (Fr. 4.4.1–4.4.9). Fr. 4.4.5 (238.1 mg) was separated by Sephadex LH-20 eluted with $CHCl_3$–MeOH (1 : 1, v/v) to yield **11** (10.0 mg). Fr. 5 (43.1 g) was further subjected to ODS CC (ϕ 4.4 × 35.0 cm) with a gradient system of MeOH–H_2O (3 : 7, 1 : 1, 6 : 4, 7 : 3 and 1 : 0, v/v) to afford 11 subfractions (Fr. 5.1–5.11). Fr. 5.2 (5.0 g) was separated by silica gel CC (ϕ 3.0 × 40.0 cm) eluted gradiently with cyclohexane–acetone (100 : 0 → 0 : 100) to yield 13 fractions (Fr. 5.2.1–5.2.13). Fr. 5.2.3 (524.3 mg) was separated by Sephadex LH-20 CC eluted with MeOH to afford 2 subfractions (Fr. 5.2.3.1–5.2.3.2). Fr. 5.2.3.1 (961.3 mg) was further purified by semipreparative RP-HPLC eluted with 25% MeCN–H_2O to yield compounds **1** (1.9 mg, t_R = 29.2 min), **2** (4.2 mg, t_R = 35.2 min) and **3** (10.2 mg, t_R = 37.0 min). Compound **2** was isolated using a chiral analytical column (35% MeCN–H_2O, 0.7 mL min^{-1}) to yield compounds **2a** (1.6 mg) and **2b** (1.6 mg). Compound **3** was isolated using a chiral analytical column (30% MeCN–H_2O, 0.7 mL min^{-1}) to yield compounds **3a** (2.3 mg) and **3b** (2.3 mg). Fr. 5.3 (1.4 g) was separated by the same manner as Fr. 5.2 to yield 10 fractions (Fr. 5.3.1–5.2.10). Fr. 5.3.6 (247.9 mg) was separated by Sephadex LH-20 CC eluted with MeOH followed by RP-HPLC eluted with 30% MeCN–H_2O to yield **14** (7.3 mg, t_R = 20.2 min). Compound **14** was isolated using a chiral analytical column (40% MeCN–H_2O, 0.7 mL min^{-1}) to yield compounds **14a** (1.5 mg) and **14b** (1.6 mg). Fr. 5.6 (8.8 g) was separated by the same manner as Fr. 5.2 to yield 10 fractions (Fr. 5.6.1–5.6.16). Fr. 5.6.10 (323.9 mg) was separated by Sephadex LH-20 CC eluted with MeOH followed by semipreparative RP-HPLC eluted with 60% MeOH–H_2O to yield compound **8** (32.0 mg, t_R = 16.2 min). Compound **8** was separated using a chiral analytical column (40% MeCN–H_2O, 0.7 mL min^{-1}) to yield compounds **8a** (0.4 mg) and **8b** (0.4 mg). Fr. 5.8 (1.2 g) was separated by silica gel CC (ϕ 2.5 × 40.0 cm) eluted gradiently with cyclohexane–acetone (100 : 0 → 0 : 100) to yield 11 fractions (Fr. 5.8.1–5.8.11). Compounds **4** (12.1 mg, t_R = 36.2 min) and **9** (13.6 mg, t_R = 60.0 min) were obtained by using semipreparative RP-HPLC eluted with 65% MeOH–H_2O from Fr. 5.8.3. Compounds **5** (31.0 mg, t_R = 35.3 min), **6** (27.9 mg, t_R = 38.3 min), **12** (19.6 mg, t_R = 43.5 min) and **13** (4.6 mg, t_R = 50.0 min) were obtained by semipreparative RP-HPLC eluted with 65% MeOH–H_2O from Fr. 5.8.4 (168.6 mg). Fr. 6 (20.6 g) was further subjected to ODS CC (ϕ 3.3 × 25.0 cm) with a gradient system of MeOH–H_2O (1 : 9, 3 : 7, 1 : 1, 7 : 3, 9 : 1 and 1 : 0, v/v) to afford 11 subfractions (Fr. 6.1–6.11). Fr. 6.4 (3.0 g) was separated by silica gel CC (ϕ 3.5 × 48.0 cm) eluted gradiently with $CHCl_3$–MeOH to yield 12 fractions (Fr. 6.4.1–6.4.12). Compounds **18** (26.1 mg, t_R = 28.5 min) and **19** (15.8 mg, t_R = 34.6 min) were obtained by using RP-HPLC eluted with 35% MeOH–H_2O from Fr. 6.4.2. (92.6 mg). Compounds **16** (20.5 mg, t_R = 35.5 min) and **17** (15.0 mg, t_R = 50.2 min) were obtained by semipreparative RP-HPLC eluted with 30% MeOH–H_2O from Fr. 6.4.4 (208.0 mg). Fr. 6.8 (1.8 g) was separated by silica gel CC (ϕ 3.5 × 57.0 cm) eluted gradiently with $CHCl_3$–acetone followed

by RP-HPLC (53% MeOH–H_2O) to yield **15** (16.7 mg, t_R = 35.5 min).

***meso*-Asarolignan A (1).** Colourless block crystals; $[\alpha]_D^{23}$ 0 (*c* 0.5, MeOH); UV (MeOH) λ_{max} (log ε) 205 (4.92), 231 (sh, 4.44), 291 nm; IR (KBr) ν_{max} 3378, 1614, 1512, 1465 cm^{-1}; ^1H and ^{13}C NMR data (Table 1); ESIMS *m*/*z* 489 $[M + Na]^+$; HRESIMS *m*/*z* 489.2094 $[M + Na]^+$ (calcd for $C_{24}H_{34}O_9Na$, 489.2101).

(+)-Asarolignan B (2a). Colourless block crystals; $[\alpha]_D^{23}$ +173.0 (*c* 0.5, MeOH); UV (MeOH) λ_{max} (log ε) 208 (4.46), 230 (4.14), 291 (3.92) nm; ECD (MeCN) λ_{max} ($\Delta\varepsilon$) 202 (+134.17), 213 (−11.41), 226 (+4.03), 240 (−16.81), 297 (+6.05) nm; IR (KBr) ν_{max} 3420, 1610, 1509, 1458 cm^{-1}; ^1H and ^{13}C NMR data (Table 1); ESIMS *m*/*z* 489 $[M + Na]^+$; HRESIMS *m*/*z* 489.2101 $[M + Na]^+$ (calcd for $C_{24}H_{34}O_9Na$, 489.2101).

(−)-Asarolignan B (2b). Colourless block crystals; $[\alpha]_D^{23}$ −174.0 (*c* 0.5, MeOH); ECD (MeCN) λ_{max} ($\Delta\varepsilon$) 203 (−127.05), 213 (+14.25), 224 (+0.52), 240 (+20.38), 298 (−4.44) nm; UV, IR, NMR, and HRESIMS were the same as those of **2a**.

(+)-Asarolignan C (3a). Light yellowish oil; $[\alpha]_D^{23}$ +167.0 (*c* 0.5, MeOH); UV (MeOH) λ_{max} (log ε) 218 (3.99) nm; ECD (MeCN) λ_{max} ($\Delta\varepsilon$) 203 (+81.57), 212 (−14.91), 225 (−2.12), 240 (−18.38), 299 (+2.13) nm; IR (KBr) ν_{max} 3421, 2931, 1735, 1653, 1073, 1029 cm^{-1}; ^1H and ^{13}C NMR data (Table 1); HRESIMS *m*/*z* 489.2103 $[M + Na]^+$ (calcd for $C_{24}H_{34}O_9Na$, 489.2101).

(−)-Asarolignan C (3b). Light yellowish oil; $[\alpha]_D^{23}$ −161.0 (*c* 0.5, MeOH); ECD (MeCN) λ_{max} ($\Delta\varepsilon$) 203 (−74.57), 212 (+0.61), 225 (−7.79), 240 (+10.05), 298 (−9.81) nm; UV, IR, NMR, and HRESIMS were the same as those of **3a**.

(±)-Asarolignan D (4). Colourless, white solid and subsequently colourless block crystals; $[\alpha]_D^{23}$ 0 (*c* 0.5, MeOH); UV (MeOH) λ_{max} (log ε) 205 (5.08), 230 (4.45), 291 (4.22) nm; IR (KBr) ν_{max} 1509, 1458 cm^{-1}; ^1H and ^{13}C NMR data (Table 2); ESIMS *m*/*z* 471 $[M + Na]^+$; HRESIMS *m*/*z* 471.2363 $[M + Na]^+$ (calcd for $C_{25}H_{36}O_7Na$, 471.2359).

(±)-Asarolignan E (5). Colourless oil; $[\alpha]_D^{23}$ 0 (*c* 0.5, MeOH); UV (MeOH) λ_{max} (log ε) 206 (5.00), 262 (4.58), 310 (4.30) nm; IR (KBr) ν_{max} 1609, 1509, 1465 cm^{-1}; ^1H and ^{13}C NMR data (Table 2); HRESIMS *m*/*z* 469.2203 $[M + Na]^+$ (calcd for $C_{25}H_{34}O_7Na$, 469.2202).

(±)-Asarolignan F (6). Colourless oil; $[\alpha]_D^{23}$ 0 (*c* 0.5, MeOH); UV (MeOH) λ_{max} (log ε) 209 (4.97), 261 (4.59), 309 (4.33) nm; IR (KBr) ν_{max} 1609, 1508, 1458 cm^{-1}; ^1H and ^{13}C NMR data (Table 2); HRESIMS *m*/*z* 469.2203 $[M + Na]^+$ (calcd for $C_{25}H_{34}O_7Na$, 469.2202).

(+)-Asarolignan G (7a). Yellowish oil; $[\alpha]_D^{23}$ +102.0 (*c* 0.5, MeOH); UV (MeOH) λ_{max} (log) 207 (5.44), 235 (4.90), 289 (4.52) nm; ECD (MeCN) λ_{max} ($\Delta\varepsilon$) 207 (+54.06), 221 (+8.25), 234 (+26.09), 285 (−3.04) nm; IR (KBr) ν_{max} 1598, 1512, 1463 cm^{-1}; ^1H and ^{13}C NMR data (Table 2); HRESIMS *m*/*z* 469.2196 $[M + Na]^+$ (calcd for $C_{25}H_{34}O_7Na$, 469.2202).

(−)-Asarolignan G (7b). Yellowish oil; $[\alpha]_D^{23}$ −106.0 (*c* 0.5, MeOH); ECD (MeCN) λ_{max} ($\Delta\varepsilon$) 207 (−30.60), 221 (−6.43), 234 (−16.74), 294 (+1.70) nm; UV, IR, NMR, and HRESIMS were the same as those of **7a**.

X-ray crystallographic analysis

Crystal data for compound (1). Data were collected using a Sapphire CCD with a graphite monochromated Mo Kα radiation, λ = 0.71073 Å at 293 K. Crystal data: $C_{24}H_{34}O_9$, M = 466.51, space group $P2_1/c$; unit cell dimensions were determined as a = 18.377(4) Å, b = 7.9014(16) Å, c = 17.239(3) Å, α = 90.00°, β = 99.43(3)°, γ = 90.00°, V = 2469.4(9) $Å^3$, Z = 4, D_x = 1.255 g m^{-3}, $F(000)$ = 1000.0, μ(Mo Kα) = 0.096 mm^{-1}. 10 765 unique reflections were collected until θ_{max} = 25.00°, in which 4347 reflections were observed [$F^2 > 4\sigma(F^2)$]. The structure was solved by direct methods using the SHELXS-97 program, and refined by the program SHELXL-97 and full-matrix least-squares calculations. In the structure refinements, non-hydrogen atoms were placed on the geometrically ideal positions by the "ride on" method. Hydrogen atoms bonded to oxygen were located by the structure factors with isotropic temperature factors. The final refinement gave R = 0.0554(3359), R_w = 0.1473(4347), S = 1.035. Crystallographic data for structure **1** has been deposited at the Cambridge Crystallographic Data Centre (CCDC 1518425).†

Crystal data for compound (2). Data were collected using a Sapphire CCD with a graphite monochromated Mo Kα radiation, λ = 0.71073 Å at 107 K. Crystal data: $C_{24}H_{34}O_9$, M = ~466, space group P_n2_1a; unit cell dimensions were determined to be a = 14.3231(5) Å, b = 23.3774(6) Å, c = 16.4367(5) Å, α = 90.00°, β = 90°, γ = 90.00°, V = 5503.6(3) $Å^3$, Z = 4, D_x = 1.267 g cm^{-3}, $F(000)$ = 2253, μ(Mo Kα) = 0.101 mm^{-1}. 33 662 reflections were collected until θ_{max} = 29.64°, in which independent unique 12 501 reflections were observed [$F^2 > 4\sigma(F^2)$]. The structure was solved by direct methods using the SHELXS-97 program, and refined by the program SHELXL-97 and full-matrix least-squares calculations. In the structure refinements, non-hydrogen atoms were placed on the geometrically ideal positions by the "ride on" method. Hydrogen atoms bonded to oxygen were located by the structure factors with isotropic temperature factors. The final refinement gave R = 0.0697(9471), R_w = 0.1815(12 501), S = 1.069, and Flack = 0.0(5). Crystallographic data for structure **2** has been deposited at the Cambridge Crystallographic Data Centre (CCDC 1518426).†

Crystal data for compound (4). Data were collected using a Sapphire CCD with a graphite monochromated Cu Kα radiation, λ = 1.54178 Å at 293 K. Crystal data: $C_{25}H_{36}O_7$, M = 448.54, space group P_12_1/c_1; unit cell dimensions were determined to be a = 11.7316(5) Å, b = 25.2812(8) Å, c = 8.4293(2) Å, α = 90.00°, β = 97.814(3)°, γ = 90.00°, V = 2476.82(14) $Å^3$, Z = 4, D_x = 1.203 g cm^{-3}, $F(000)$ = 968, μ(Cu Kα) = 0.710 mm^{-1}. 11 344 reflections were collected until θ_{max} = 62.72°, in which independent unique 3954 reflections were observed [$F^2 > 4\sigma(F^2)$]. The structure was solved by direct methods using the SHELXS-97 program, and refined by the program SHELXL-97 and full-matrix least squares calculations. In the structure refinements, non-hydrogen atoms were placed on the geometrically ideal positions by the "ride on" method. Hydrogen atoms bonded to oxygen were located by the structure factors with isotropic temperature factors. The final refinement gave R = 0.0478(3012), R_w = 0.1338(3954), S = 1.040. Crystallographic

data for structure **4** has been deposited at the Cambridge Crystallographic Data Centre (CCDC 1518427).†

Crystal data for compound (8). Data were collected using a Sapphire CCD with a graphite monochromated Cu Kα radiation, $\lambda = 1.54180$ Å at 293 K. Crystal data: $C_{22}H_{24}O_6$, $M = 384.41$, space group P_12_1/n_1; unit cell dimensions were determined to be $a = 7.5710(2)$ Å, $b = 15.1433(4)$ Å, $c = 17.5456(5)$ Å, $\alpha = 90.00°$, $\beta = 91.007(3)°$, $\gamma = 90.00°$, $V = 2011.29(10)$ Å^3, $Z = 4$, $D_x = 1.269$ g cm^3, $F(000) = 816$, μ(Cu Kα) $= 0.759$ mm^{-1}. 8905 reflections were collected until $\theta_{max} = 62.76°$, in which independent unique 3208 reflections were observed [$F^2 > 4\sigma(F^2)$]. The structure was solved by direct methods using the SHELXS-97 program, and refined by the program SHELXL-97 and full-matrix least-squares calculations. In the structure refinements, nonhydrogen atoms were placed on the geometrically ideal positions by the "ride on" method. Hydrogen atoms bonded to oxygen were located by the structure factors with isotropic temperature factors. The final refinement gave $R = 0.0382$, $R_w = 0.1016$, $S = 1.055$. Crystallographic data for structure **8** has been deposited at the Cambridge Crystallographic Data Centre (CCDC 1518428).†

ECD calculation method

In theoretical calculations, the geometry of the molecules was optimized with Gaussian 09 package 33 at B3LYP/6-31G(d) computational level. The minimum nature of the structure was confirmed by frequency calculations at the same computational level. Then ECD calculations were carried out in the methyl cyanide solvent medium using time-dependent density functional theory (TDDFT) with B3LYP functional and DGDZVP basis set.

Anti-neuroinflammatory activity assays

BV-2 cells were obtained from Peking Union Medical College (PUMC) Cell Bank (Beijing, People's Republic of China) and were maintained at 5×10^5 cells per mL in DMEM medium supplemented with 10% heat-inactivated FBS, penicillin G (100 U mL^{-1}), streptomycin (100 mg L^{-1}), and L-glutamine (2 mM), and they were incubated at 37 °C in a humidified atmosphere containing 5% CO_2. The cell viability was determined by adding 0.8 mL of CCK-8 to each well and incubated at 37 °C for 4 h. Then, the OD value was read at 450 nm using a Bio-Rad ELISA microplate reader.

To measure TNF-α production, cells were seeded in a 96-well plate at a density of 1.5×10^6 cells per well in DMEM and incubated for 24 h. The cultures were prepared and stimulated with LPS (1 μg mL^{-1}) in the presence or absence of LNE. Thereafter, the cells were treated with 5, 20 and 50 μM concentrations of **1–23** respectively. The purity of compound **10** is 94.7%, the purity of compound **13** is 90.1%, the purity of other compounds range from 95.0% to 99.0% (see ESI†). After 24 h incubation, supernatant from the culture medium was harvested and used for measuring the level of TNF-α. TNF-α were measured by using an ELISA kit.

Acknowledgements

This work was supported by grants from the National Natural Science Foundation of China (81422054, 81172945), and the support from State Key Laboratory of Bioactive Substance and Function of Natural Medicines (GTZK201505), the Guangdong Natural Science Funds for Distinguished Young Scholar (S2013050014287).

Notes and references

1 X. L. Feng, Y. Yu, D. P. Qin, H. Gao and X. S. Yao, *RSC Adv.*, 2015, **5**, 5173–5182.
2 J. Mao, S. Huang, S. Liu, X. L. Feng, M. Yu, J. Liu, Y. E. Sun, G. L. Chen, Y. Yu, J. Zhao and G. Pei, *Aging Cell*, 2015, **14**, 784–796.
3 Z. Q. Li, G. P. Zhao, S. Q. Qian, Z. J. Yang, X. Y. Chen, J. Chen and C. Cai, *J. Ethnopharmacol.*, 2012, **144**, 305–312.
4 H. Y. Qi, L. Chen, L. Ning, H. Ma, Z. Y. Jiang, Y. Fu and L. Li, *J. Pharm. Biomed. Anal.*, 2015, **115**, 292–299.
5 M. Sundaramahalingam and S. D. Rathinasamy, *Pharmacol. Res.*, 2005, **52**, 467–474.
6 G. Wei, Y. B. Chen, D. F. Chen, X. P. Lai, D. H. Liu and R. D. Deng, *J. Alzheimer's Dis.*, 2013, **33**, 863–880.
7 B. W. Kim, S. Koppula, H. Kumar, J. Y. Park, I.-W. Kim, S. V. More, I.-S. Kim, S. D. Han and S. K. Kim, *Neuropharmacology*, 2015, **97**, 46–57.
8 C. Ranjithkumar, P. Vijayapandi and M. Zahurin, *Front. Pharmacol.*, 2016, **7**, 72/1–72/8.
9 Y. Y. Lu, Y. B. Xue, S. J. Chen, H. C. Zhu, J. W. Zhang, X. N. Li, J. P. Wang, J. J. Liu, C. X. Qi, G. Du and Y. H. Zhang, *Sci. Rep.*, 2016, **6**, 22909/1–22909/10.
10 G. Ni, *Study on chemical constituents and bioactivities and of Acorus tatarinowii and Morus cathayana*, Chinese Academy of Medical Sciences and Peking Union Medical College, People Rep China, 2010.
11 J. H. Ryu, H. J. Son, S. H. Lee and D. H. Sohn, *Bioorg. Med. Chem. Lett.*, 2002, **12**, 649–651.
12 S. Kadota, K. Tsubono, K. Makino, M. Takeshita and T. Kikuchi, *Tetrahedron Lett.*, 1987, **28**, 2857–2860.
13 T. Kikuchi, S. Kadota, K. Yanada, K. Tanaka, K. Watanabe, M. Yoshizaki, T. Yokoi and T. Shingu, *Chem. Pharm. Bull.*, 1983, **31**, 1112–1114.
14 X. G. Tong, G. S. Wu, C. G. Huang, Q. Lu, Y. H. Wang, C. L. Long, H. R. Luo, H. J. Zhu and Y. X. Cheng, *J. Nat. Prod.*, 2010, **73**, 1160–1163.
15 G. Ni, Z. F. Shen, Y. Lu, Y. H. Wang, Y. B. Tang, R. Y. Chen, Z. Y. Hao and D. Q. Yu, *J. Org. Chem.*, 2011, **76**, 2056–2061.
16 N. Matsuda and M. Kikuchi, *Chem. Pharm. Bull.*, 1996, **44**, 1676–1679.
17 Z. Yuan and X. Li, *Chin. J. Magn. Reson.*, 2003, **20**, 307–314.
18 C. H. Park, K. H. Kim, I. K. Lee, S. Y. Lee, S. U. Choi, J. H. Lee and K. R. Lee, *Arch. Pharmacal Res.*, 2011, **34**, 1289–1296.
19 A. Patra and A. K. Mitra, *J. Nat. Prod.*, 1981, **44**, 668–669.

20 T. D. Silva and L. M. X. Lopes, *Phytochemistry*, 2006, **67**, 929–937.
21 L. M. X. Lopes, M. Yoshida and O. R. Gottlieb, *Phytochemistry*, 1982, **21**, 751–755.
22 C. K. Johnathan, K. Janine, F. Laura, R. H. Paul, R. Magnus and J. S. Pamela, *Nat. Rev. Neurol.*, 2012, **8**, 518–530.
23 X. Jiang, L. Chen, L. L. Shen, Z. W. Chen, L. X. Xu, J. J Zhang and X. F Yu, *Brain Res.*, 2016, **1649**, 30–37.
24 V. Barbara, B. Mariaserena, M. Natalia and M. Marina, *Neurotoxicology*, 2014, **43**, 10–20.